

Group-velocity dispersion measurements of water, seawater, and ocular components using multiphoton intrapulse interference phase scan

Yves Coello,¹ Bingwei Xu,¹ Tricia L. Miller,² Vadim V. Lozovoy,¹ and Marcos Dantus^{1,*}

¹Department of Chemistry, Michigan State University, East Lansing, Michigan 48824, USA

²BioPhotonic Solutions, Inc., Okemos, Michigan 48864, USA

*Corresponding author: dantus@msu.edu

Received 19 July 2007; accepted 14 October 2007;
posted 25 October 2007 (Doc. ID 85350); published 3 December 2007

The use of femtosecond lasers requires accurate measurements of the dispersive properties of media. Here we measure the second- and third-order dispersion of water, seawater, and ocular components in the range of 660–930 nm using a new method known as multiphoton intrapulse interference phase scan. Our direct dispersion measurements of water have the highest precision and accuracy to date. We found that the dispersion for seawater increases proportionally to the concentration of salt. The dispersion of the vitreous humor was found to be close to that of water. The chromatic dispersion of the cornea–lens complex was measured to obtain the full dispersive properties of the eye. © 2007 Optical Society of America

OCIS codes: 320.0320, 170.7160, 010.0010.

1. Introduction

The growing number of femtosecond lasers in industry, medicine, and communications has increased the need for measuring the dispersive properties of media beyond that of glass and quartz. Because of their broad bandwidth, femtosecond lasers are particularly sensitive to chromatic-dispersion characteristics of materials, in particular second-order (k'') and third-order dispersion (k'''), which typically cause pulse broadening.

Pulse duration is a very important parameter in femtosecond laser applications, for example, laser micromachining and laser eye surgery, because it determines the peak power density available to ablate the material. If substantial broadening takes place, the ability of the laser to achieve consistent ablation is greatly diminished. In this paper we carry out direct measurements on the chromatic dispersion of water, seawater, and ocular components.

Femtosecond lasers are routinely used for opening the corneal flap in the bladeless LASIK technique. A

number of additional procedures are currently under investigation. *In vitro* experiments have shown that femtosecond laser ablation may be useful for the treatment of glaucoma by making channels through the trabecular meshwork in the eye without damaging the surrounding tissue. These channels provide a pathway for the release of fluid and may result in a significant intraocular pressure reduction *in vivo* [1]. Femtosecond laser surgery on retinal lesions appears to be a promising treatment for macular degeneration [2]. More recently, intratissue multiphoton ablation in the cornea has been demonstrated opening the possibility of treating visual disorders without the need of corneal flaps as used for LASIK [3]. Femtosecond laser cuts in the lens without damaging adjacent tissue is being developed for the treatment of presbyopia, a very common disease with no satisfactory treatment currently available [4,5].

All the applications above can be greatly improved using the shortest femtosecond laser pulses, taking advantage of the reduced energy required to achieve a specific peak power density. Less energy implies less collateral damage to healthy tissue. However, sub-50 fs pulses undergo significant broadening by transmitting through optical media including ocular

components. Therefore, accurate dispersion measurements and a means to eliminate phase distortions, as presented here, will be required to consistently achieve the best results. Conversely, from the point of view of laser eye safety, femtosecond pulses that achieve their shortest duration at the retina pose the greatest risk [6].

Here we report on the use of multiphoton intrapulse interference phase scan (MIIPS) [7–10], a relatively novel method capable of directly measuring chromatic dispersion (ϕ'') of a broad variety of media. The method is based on the dependence of nonlinear optical processes such as second-harmonic generation (SHG) from the spectral phase of a broad-bandwidth femtosecond laser pulse [8,11] and requires a means to apply calibrated wavelength-dependent phases on the laser pulses. We used MIIPS to measure the second-order dispersion k'' of de-ionized water and compared it to literature values. We then measured the dependence of k'' on the concentration of sea salt in water and k'' of the ocular vitreous humor. Finally we measured ϕ'' of the cornea–lens complex. These two eye components together, the vitreous humor and the cornea–lens complex, account for all the transparent parts of the eye.

2. Dispersion Measurements Using MIIPS

We start our discussion by remembering that the wavenumber is defined by $k \equiv \omega n(\omega)/c \equiv 2\pi n(\lambda)/\lambda$, where ω is the angular frequency of light, n is the refractive index of the medium, c is the speed of light in vacuum, and λ is the free-space wavelength of light. The phase retardation that light with frequency ω experiences is given by $\phi(\omega) = k(\omega)z$, where z is the path length traveled by the light. As a broad-bandwidth femtosecond laser pulse propagates, it undergoes chromatic dispersion ($\phi'' \equiv d^2\phi/d\omega^2$), second-order dispersion ($k'' \equiv d^2k/d\omega^2$), and third-order dispersion ($k''' \equiv d^3k/d\omega^3$). For a Gaussian pulse the second-order dispersion k'' is equal to the group-velocity dispersion (GVD) $\equiv d(1/v_g)/d\omega$, where v_g is the group velocity [12]. The chromatic dispersion ϕ'' for a Gaussian pulse is also known as group-delay dispersion (GDD).

Another common definition of GVD is the derivative of the group velocity with respect to wavelength $dv_g/d\lambda$. This is sometimes a source of confusion because the strictest definition of GVD is $dv_g/d\omega$. According to either of these definitions the GVD and GDD are not only functions of the media but also functions of the shape of the envelope of the field. Here we measure ϕ'' and k'' , which depend on the media only.

While the refractive index of materials can be directly measured using a hollow prism arrangement [13], the measurement of k'' is more difficult. It can be calculated using an analytical formula for the index of refraction according to

$$k''(\lambda) = \frac{\lambda^3}{2\pi c^2} \frac{d^2n(\lambda)}{d\lambda^2}. \quad (1)$$

However, because derivatives are very sensitive to noise and more importantly depend on the phenomenological formula used to fit the data, this indirect method has unpredictable precision and accuracy. One of the most accurate methods used to measure dispersive properties is white-light interferometry, where an interferometer is constructed using a broad-bandwidth source of light and the material is introduced in one of the arms [14]. In this case, the phase distortions introduced in the sample arm can be measured directly, and usually after decomposition in a Taylor series, the second derivative ϕ'' can be extracted. There is also a variety of time-of-flight, phase-shift, interferometric measurement techniques [15]. These methods are limited by their temporal resolution and are time consuming because they depend on wavelength and/or time scans.

MIIPS directly measures ϕ'' from the dependence of the SHG spectrum of the laser pulses on the spectral phase. The phase dependence of the SHG signal at frequency 2ω for a pulse with phase modulation $\phi(\omega)$ can be approximated by

$$\begin{aligned} \text{SHG}(2\omega) &\propto \left| \int E(\omega + \Omega)E(\omega - \Omega)d\Omega \right|^2 \\ &\approx \left| \int e^{i\phi(\omega+\Omega) + i\phi(\omega-\Omega)} d\Omega \right|^2, \end{aligned} \quad (2)$$

where E is the electric field and Ω is a dummy integration variable that takes into account frequency components detuned from ω . If we expand $\phi(\omega)$ in a Taylor series, we find that the zeroth- and first-order terms vanish, leaving

$$\text{SHG}(2\omega) \propto \left| \int e^{i\phi''(\omega)\Omega^2} d\Omega \right|^2, \quad (3)$$

an approximation that is good for smooth phase functions. Phase modulation causes a maximum in the SHG spectrum at the frequencies where $\phi''(\omega) = 0$.

For MIIPS, a set of reference sinusoidal phase functions, for example, $f(\omega, \delta) = \alpha \sin[\gamma(\omega - \omega_0) - \delta]$, is applied to the pulses, where γ is chosen so that one full period of the function encompasses the spectrum of the pulse (see Fig. 1), and δ is a parameter that is scanned across a 4π rad range. Each reference function $f(\omega, \delta)$ causes the SHG spectrum to show a single maximum that is centered at the position where $\phi''(\omega) = 0$. For a pulse without phase distortions, known as a transform-limited (TL) pulse, the maximum occurs where the sinusoidal phase function has a point of inflection ($f''(\omega, \delta) = 0$), as it is illustrated in Fig. 1. The collection of SHG spectra as a function of δ results in a two-dimensional contour plot with diagonal features that correspond to the maximum amplitude of the SHG spectra. The MIIPS traces in Fig. 2(a) correspond to TL pulses.

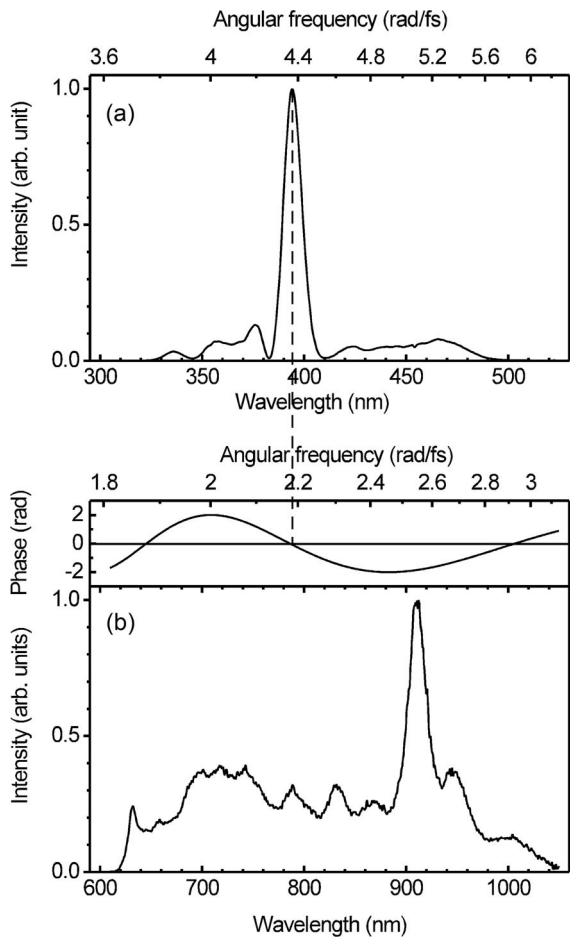


Fig. 1. Sinusoidal spectral phase function in the frequency domain produces a maximum in the SHG spectrum at the frequency corresponding to the point of inflection of the spectral phase. (b) Spectrum of the ultrabroad-bandwidth femtosecond laser used for this work. (a) The experimental SHG spectrum obtained when the sinusoidal spectral phase shown in (b) (top) is applied to the laser pulses.

When an initially TL pulse propagates through a medium, it acquires spectral phase distortions $\phi(\omega)$, which can be accurately measured using MIIPS. The overall spectral phase of the pulses after propagating through media and applying a phase $f(\omega, \delta)$ is then $\phi_{\text{total}}(\omega) = \phi(\omega) + f(\omega, \delta)$. The condition for the maximum in the SHG spectrum is now $\phi''_{\text{total}}(\omega) = \phi''(\omega) + f''(\omega, \delta_{\text{max}}) = 0$, where δ_{max} is the value of the parameter δ for which the measured SHG at frequency 2ω is maximized. Because we know the second derivative of the function $f(\omega, \delta)$ added by the pulse shaper, we can easily calculate the chromatic dispersion using

$$\phi''(\omega) = -f''(\omega, \delta_{\text{max}}) = \alpha\gamma^2 \sin[\gamma(\omega - \omega_0) - \delta_{\text{max}}(\omega)]. \quad (4)$$

The second-order component of the phase distortions causes a change in the spacing between the MIIPS features, as shown in Fig. 2(b), while the third-order

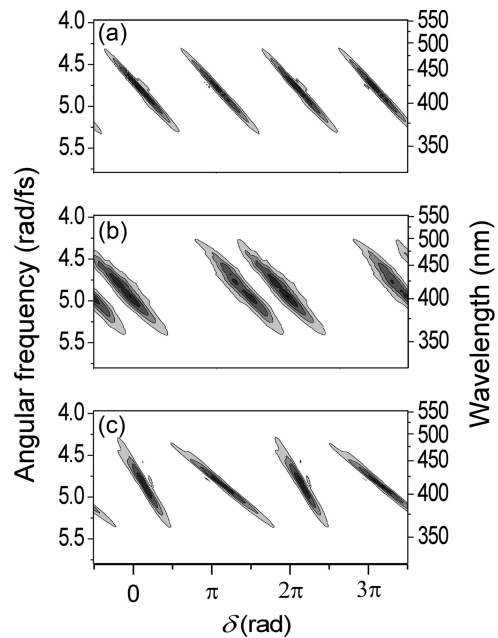


Fig. 2. (a) Experimental MIIPS traces for TL pulses. Diagonal features are equally spaced and have the same slope. (b) Experimental MIIPS traces showing the change in spacing between the diagonal features caused by a $\phi'' = 120 \text{ fs}^2$ quadratic phase distortion in the frequency domain. (c) Experimental MIIPS traces showing the slope change caused by a $\phi''' = 336 \text{ fs}^3$ cubic phase distortion in the frequency domain.

component of the phase distortions causes a change in the slope of the features, as shown in Fig. 2(c).

In white-light interferometry [16], interference $I(\omega)$ occurs between the reference field $E_0(\omega)$ and the field after propagating through the sample $E_0(\omega) \exp[i\phi(\omega)]$. The spectral phase function $\phi(\omega)$ can be extracted using the interference term $I(\omega) \propto I_0(\omega) \cos[\phi(\omega)]$. The chromatic dispersion is then calculated by taking the appropriate derivatives. MIIPS has built-in interferometric accuracy. We measure the SHG at frequency 2ω , where interference occurs between the fields $E(\omega - \Omega)$ and $E(\omega + \Omega)$ [see formula (2)]. In this case, the chromatic dispersion ϕ'' can be directly obtained from the position of the spectral maximum using Eq. (4).

A complete theoretical discussion of MIIPS is outside the scope of this publication. For an in-depth discussion of the precision and accuracy of MIIPS measurements of spectral phase distortions, the reader is referred to the comprehensive paper by Xu *et al.* [9] and the review by Lozovoy and Dantus [8].

3. Experimental

For this work we used an ultrabroad-bandwidth femtosecond Ti:Al₂O₃ laser oscillator with chirped mirrors, whose spectrum spans 620–1050 nm [spectrum is shown in Fig. 1(b)] and that was used to generate the broadest SHG spectrum to date [17]. This laser system provides measurements of chromatic dispersion in the very broad spectral range without tuning the laser or realigning the optical system.

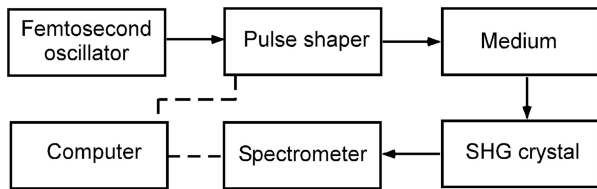


Fig. 3. Block diagram of the experimental setup. The arrows indicate the propagation of the laser beam, the dashed lines indicate computer communication.

The pulse shaper used for our work was a folded all-reflective grating-based system described in an earlier publication [17]. The main elements of the shaper are a 150 lines/mm grating, a 762 mm focal-length spherical mirror, and a 640 pixel dual-mask spatial light modulator (SLM-640, CRi Incorporated). After the shaper, the pulses were focused onto a 20 μm type-I KDP crystal, and the SHG signal was separated from the fundamental before it was directed to a spectrometer (QE65000, Ocean Optics Incorporated). A block diagram of the experimental setup is shown in Fig. 3.

Before making the measurements, it is important that phase distortions, including those introduced by empty glass cuvettes or slides, are eliminated. This is

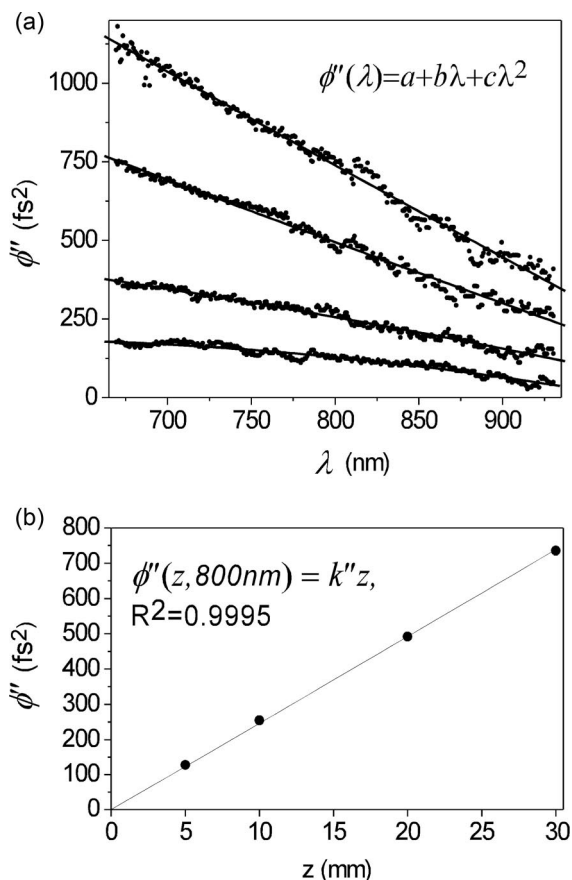


Fig. 4. Chromatic dispersion as a function of medium thickness. (a) $\phi''(\lambda)$ data points measured by MIIPS and second-order polynomial fits for water samples of 5, 10, 20, and 30 mm thickness (ascending order). (b) Linear regression of $\phi''(\lambda)$ at 800 nm.

a simple task. MIIPS can measure $\phi''(\omega)$, therefore one can calculate the phase distortions $\phi(\omega)$ after double integration and use the pulse shaper to introduce a phase that cancels the phase distortions by subtraction, $-\phi(\omega)$ [9,17]. Once the phase distortions of the system are eliminated, the desired medium with thickness z is introduced, and its chromatic dispersion ϕ'' as function of wavelength or frequency is measured using MIIPS. This measurement is presented in Fig. 4 for the case of different path lengths of water. The lines in Fig. 4 correspond to a fit of the experimental data set containing hundreds of points to $\phi''(\lambda) = a + b\lambda + c\lambda^2$. We confirmed that the results are independent from the fitting function selected. In the MIIPS measurements of ϕ'' we used $\gamma = 6$ fs and $\alpha = 2\pi$ [see formula (4)]. For large phase distortions, the first MIIPS iterations were carried out with larger α values (up to 10π), and, as the distortions were eliminated, α was reduced. The δ parameter was scanned across the 4π rad range in 128 steps.

Given that the chromatic dispersion varies linearly with the sample thickness, $\phi'' = k''z$, the second-order dispersion $k''(\lambda)$ was calculated from the slope of the dependence at each wavelength [Fig. 4(b)]. The error bars reported for k'' correspond to the standard deviation of the slopes for three sets of independent experiments.

De-ionized water with a room-temperature mean conductivity of 2 $\mu\text{S}/\text{cm}$ was used in all cases. Artificial seawater was prepared by dissolving instant Ocean sea salt in de-ionized water with concentrations of 35.8 and 107.4 g/l for the 1 \times and 3 \times samples, respectively. Four glass cuvettes with path lengths of 5, 10, 20, and 30 mm were used for the

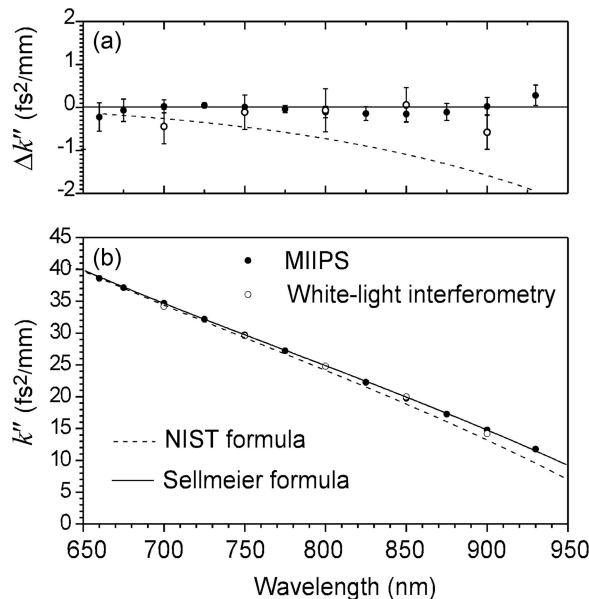


Fig. 5. Comparison of k'' for water measured by MIIPS and white-light interferometry and calculated using the Sellmeier and NIST dispersion formulas. The upper graph shows the difference of the corresponding values with respect to those calculated using the Sellmeier dispersion formula. For both calculations a temperature of 21.5 $^{\circ}\text{C}$ was used.

Table 1. Parameters of the Sellmeier Formula for Water at 21.5 °C

i	A_i	λ_i (nm)
1	0.5689093832	71.486374884
2	0.1719708856	135.099228532
3	0.02062501582	161.992558595
4	0.1123965424	3267.269774598

water and seawater measurements. Fresh (uncured) adult approximately 18 month old Holstein cow eyes, that would have otherwise been discarded, were obtained from a slaughterhouse. The vitreous humor was extracted and three glass cuvettes with path lengths of 5, 10, and 20 mm were used for the measurements. A cow cornea–lens complex was extracted and squeezed to approximately 5 mm thickness with glass slides for the measurements.

4. Results

A. Chromatic Dispersion of De-Ionized Water

Measurements of $k''(\lambda)$ are presented in Fig. 5 together with a comparison to earlier measurements and results of calculations based on the knowledge of the index of refraction as a function of frequency. The black dots represent our measurements, the open dots represent measurements using white-light interferometry [18], the solid curves correspond to the calculated $k''(\lambda)$ values based on a Sellmeier approximation for the refractive index of distilled water [13], and the dashed curves correspond to the calculated $k''(\lambda)$ values based on a polynomial formula for the refractive index of water adopted by the National Institute of Standards and Technology (NIST) of the United States [19].

Figure 5(a) shows the deviation of the experimental measurements from the calculated dispersion based on the Sellmeier formula (line). Below we provide the Sellmeier formula (5) and the parameters provided by Daimon and Masumura [13] used for our calculations of k'' using formula (1):

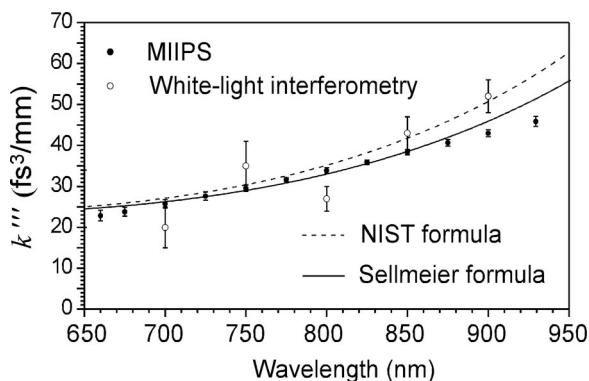


Fig. 6. Comparison of water third-order dispersion calculated from our measurements, the Sellmeier and NIST dispersion formulas, and obtained using white-light interferometry.

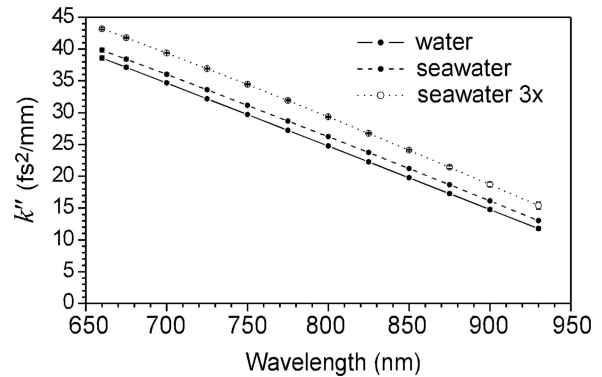


Fig. 7. Experimental measurements of k'' of water, seawater, and water with three times the concentration of salt in seawater (3 \times). Only a few experimental points were plotted for clarity.

$$n^2 - 1 = \sum_{i=1}^4 \frac{A_i}{1 - (\lambda_i/\lambda)^2}, \quad (5)$$

where A_i and λ_i can be associated with effective resonances and are collected in Table 1. Experimental values of k'' for water at selected wavelengths are shown in Table 4.

Based on the measured second-order dispersion we can calculate the third-order dispersion as $k'''(\omega) = dk''/d\omega$. The result of this calculation is presented in Fig. 6 together with the corresponding measurements by white-light interferometry [18] and the calculation based on the Sellmeier [13] and NIST dispersion formulas [19].

B. Chromatic Dispersion of Seawater

A difference between the k'' s of water and seawater was measured, and the results are shown in Fig. 7. Furthermore, we found that the increase in k'' when salt is added, $\Delta k''(S) = k''(S) - k''(S = 0)$ is directly proportional to the salinity (S) and independent from wavelength. This direct proportionality can also be derived from the formula for the refractive index of seawater proposed by Quan and Fry [20]. They fit

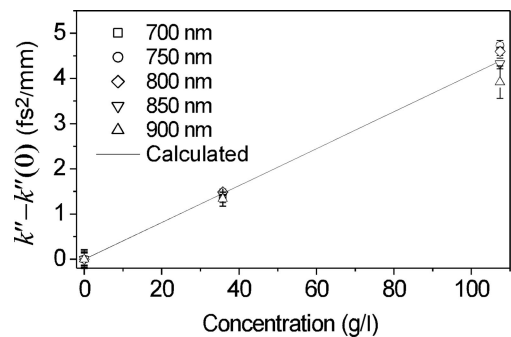


Fig. 8. Increase in k'' of seawater with respect to de-ionized water as a function of the concentration of sea salt. The symbols correspond to MIIPS measurements and the line to a calculation based on the refractive index formula for seawater proposed by Quan and Fry [20]. For the calculation the temperature was set at 21.5 °C. Note that the calculation has been extended beyond the original range of validity for S (~ 35 g/l).

Table 2. Seawater Parameters for Eq. (6) in the 660–930 nm Range

C_0	$102.42174 \pm 0.46809 \text{ fs}^2 \text{ mm}^{-1}$
C_1	$-0.09476 \pm 0.00118 \text{ fs}^2 \text{ mm}^{-1} \text{ nm}^{-1}$
C_2	$-2.88686 \times 10^{-6} \pm 0.74132 \times 10^{-6} \text{ fs}^2 \text{ mm}^{-1} \text{ nm}^{-2}$
C_S	$0.04008 \pm 0.00157 \text{ fs}^2 \text{ mm}^{-1} \text{ g}^{-1} \text{ l}$

the experimental refractive index data for seawater measured by Austin and Halikas [21] to a ten-term empirical formula in the wavelength range of 400–700 nm and salinity range of 0–35 g/l. The resulting formula contains only one term proportional to S and λ ($n(\lambda) \propto S/\lambda$). Since $k''(\lambda) \propto \lambda^3 d^2 n(\lambda)/d\lambda^2$ the formula predicts that $\Delta k''(S)$ is directly proportional to S and independent of λ . In Fig. 8, we compare the effect of salinity on k'' measured by MIIPS with that calculated using the refractive index formula for seawater in [20].

There seems to be a need for a formula that correctly predicts the wavelength and salinity dependence of k'' . We propose that $k''(\lambda)$ can be expressed as

$$k''(\lambda) = C_0 + C_1\lambda + C_2\lambda^2 + C_S S, \quad (6)$$

where the coefficients C_0 , C_1 , and C_2 were calculated from experimental data for de-ionized water (see Fig. 7) and the coefficient C_S was calculated using a linear regression for $\Delta k''(S)$ (see Fig. 8). The parameters of the fit are given in Table 2. These values and the errors were calculated using the ORIGIN 6.1 software (OriginLab Corporation). Experimental values of k'' for seawater at selected wavelengths are shown in Table 4.

C. Chromatic Dispersion of the Vitreous Humor and the Cornea–Lens Complex

Ocular dispersion data are particularly scarce for near-infrared wavelengths [22,23]. To help remedy this lack of information we measured the dispersive properties of all the transparent components of the eye, the cornea–lens complex, and the vitreous humor (Fig. 9).

We found that the second-order dispersion k'' of the vitreous humor is very close to that of water, as is shown in Fig. 10. The data were fit to a second-order

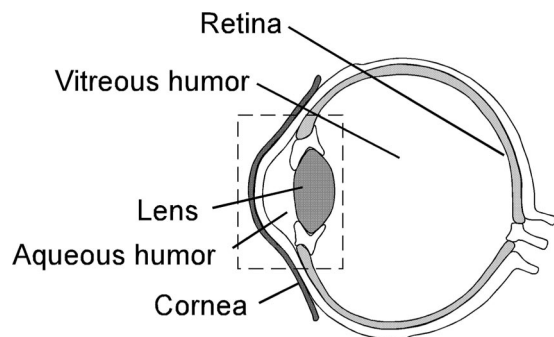


Fig. 9. Diagram of an eye. The dashed square corresponds to the cornea–lens complex.

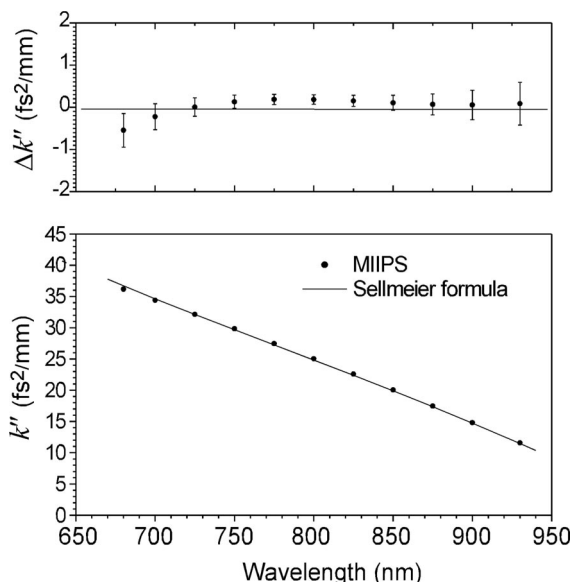


Fig. 10. Comparison of k'' for the vitreous humor measured by MIIPS and k'' for water calculated using the Sellmeier dispersion formula for distilled water. The upper graph shows the deviation of the vitreous humor measurements with respect to the calculated values for water.

polynomial [Eq. (7)]. The parameters of the fit are shown in Table 3. Experimental measurements of k'' for the vitreous humor at selected wavelengths are shown in Table 4:

$$k''(\lambda) = C_0 + C_1\lambda + C_2\lambda^2. \quad (7)$$

The measured chromatic dispersion ϕ'' of a cornea–lens complex is shown in Fig. 11. For this experiment we were not able to use different path lengths. The data presented come from a set of three measurements on the same tissue. Values of ϕ'' for the cornea–lens complex at selected wavelengths are shown in Table 4. From our data we obtain a value of 33 fs^2/mm for $k''(\lambda = 800 \text{ nm})$.

5. Discussion

A. Chromatic Dispersion of De-Ionized Water and Seawater

Analysis of our experimental results for water clearly shows excellent agreement with the calculations based on the Sellmeier model [Eq. (5)]. The deviation between our measurements and the calculated values based on this model are smaller than 0.2 fs^2/mm within the measured wavelength range, and for some of the points, the deviation is even lower than 0.1 fs^2/mm . Note that using the refractive index for-

Table 3. Vitreous Humor Parameters for Eq. (7) in the 660–930 nm Range

C_0	$76.04648 \pm 1.52198 \text{ fs}^2 \text{ mm}^{-1}$
C_1	$-0.02954 \pm 0.00382 \text{ fs}^2 \text{ mm}^{-1} \text{ nm}^{-1}$
C_2	$-4.27553 \times 10^{-5} \pm 0.239476 \times 10^{-5} \text{ fs}^2 \text{ mm}^{-1} \text{ nm}^{-2}$

Table 4. Experimental Dispersion Measurements for Water, Seawater, and Eye Components

Wavelength (nm)	Water k'' (fs ² /mm)	Seawater k'' (fs ² /mm)	Vitreous Humor k'' (fs ² /mm)	Cornea–Lens ϕ'' (fs ²)
660	38.62 ± 0.33	39.85 ± 0.31	—	—
675	37.14 ± 0.26	38.42 ± 0.26	36.63 ± 0.42	—
700	34.67 ± 0.15	36.03 ± 0.19	34.42 ± 0.31	203 ± 7
725	32.20 ± 0.06	33.61 ± 0.14	32.16 ± 0.22	183 ± 2
750	29.72 ± 0.02	31.18 ± 0.09	29.84 ± 0.16	172 ± 1
775	27.25 ± 0.08	28.72 ± 0.06	27.47 ± 0.12	167 ± 2
800	24.76 ± 0.13	26.25 ± 0.04	25.05 ± 0.11	164 ± 1
825	22.28 ± 0.16	23.75 ± 0.03	22.58 ± 0.13	161 ± 1
850	19.79 ± 0.18	21.23 ± 0.03	20.05 ± 0.18	153 ± 1
875	17.29 ± 0.20	18.69 ± 0.05	17.47 ± 0.25	137 ± 1
900	14.80 ± 0.21	16.14 ± 0.09	14.83 ± 0.35	111 ± 4
930	11.79 ± 0.24	13.04 ± 0.14	11.60 ± 0.51	—

mula adopted by NIST to calculate the second-order dispersion leads to values that considerably deviate from experimental measurements and calculations based on Eq. (5). We conclude that MIIPS provides precision and accuracy at least two times better than white-light interferometry.

There is also a surprisingly good agreement between our experimental measurements for seawater and the calculations based on the formula for the refractive index of seawater in [20], considering that this was derived for a different range of wavelengths and for a much smaller range of salinity.

B. Chromatic Dispersion of the Vitreous Humor and the Cornea–Lens Complex

Having measured the chromatic dispersion of the ocular components, we can now predict pulse broadening. If an initial TL Gaussian pulse of time duration τ_0 and centered at λ_0 acquires a chromatic dispersion $\phi'' = \phi''(\lambda_0)$ after propagating through a dispersive medium, then its final pulse duration [12] is

$$\tau = \tau_0 [1 + (4\phi''\tau_0^{-2} \ln 2)^2]^{0.5}. \quad (8)$$

For a human eyeball we estimate that $\phi'' = k''_h z + \phi''_c$, where k''_h is the second-order dispersion of the vitreous humor, $z = 20$ mm is the path length that

light travels inside the vitreous humor, and ϕ''_c is the chromatic dispersion of the cornea–lens complex. For initial 10 and 50 fs TL pulses centered at 800 nm, using Table 4 and Eq. (8), we find that $\phi'' \approx 665$ fs² and that the pulse durations at the retina would be 185 and 62 fs, respectively. From this, we can also learn that sub-50 fs pulses with $\phi'' \approx -665$ fs² pose the greatest eye laser safety risk.

Pulse broadening is important because peak power densities at the target are inversely proportional to the time duration of the pulses. For example, if one focuses a 10 fs 1 μ J pulse to 10 μ m², the peak power density would be 10¹⁵ W/cm². This extreme power density causes the desired localized ablation without collateral damage. If the time duration increases ten times, the peak intensity is reduced by an order of magnitude, and the ablation ability of the pulses decreases.

We want to point out that we performed calculations of k'' for human vitreous humor based on several proposed refractive index formulas [23–25]. These calculations lead to values of $k''(\lambda = 800$ nm) that deviate from 7 to 20 fs²/mm from our experimental measurements at 800 nm. The difference between measured and calculated values comes from the fact that the k'' calculation is highly dependent on the formula used to fit the refractive index data [see Eq. (1)].

6. Conclusion

We introduce a new direct method to measure the chromatic dispersion of transparent media. Comparison of our data with other measurements suggests that the accuracy and precision of our method are the most reliable to date. Knowledge of the reported chromatic dispersion measurements of water and seawater is necessary for laser propagation models in these media. The chromatic dispersion for ocular components will be useful for laser eye surgery and laser safety data guidelines. The measurement and elimination of chromatic dispersion (second and higher orders) as shown here, using MIIPS, is highly recommended for the highest reliability and reproducibility of applications using femtosecond pulses.

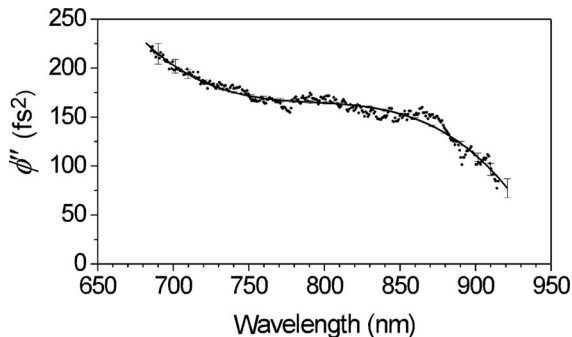


Fig. 11. Measured chromatic dispersion ϕ'' of a cornea–lens complex. The dots correspond to the experimental points. The curve corresponds to a third-order polynomial fit of the data.

We gratefully acknowledge funding for this research from the National Science Foundation, Major Research Instrumentation grant CHE-0421047. T. L. Miller thanks BioPhotonic Solutions, Inc. for allowing her to participate in this research project.

References

1. S. Toyran, Y. M. Liu, S. Singha, S. Shan, M. R. Cho, R. J. Gordon, and D. P. Edward, "Femtosecond laser photodisruption of human trabecular meshwork: an in vitro study," *Exp. Eye Res.* **81**, 298–305 (2005).
2. T. M. Johnson and B. M. Glaser, "Micropulse laser treatment of retinal-choroidal anastomoses in age-related macular degeneration," *Graefes Arch. Ophthalmol.* **243**, 570–575 (2005).
3. B. G. Wang, I. Riemann, H. Schubert, K. J. Halhuber, and K. Koenig, "In-vivo intratissue ablation by nanjoule near-infrared femtosecond laser pulses," *Cell Tissue Res.* **328**, 515–520 (2007).
4. M. Blum, K. Kunert, S. Nolte, S. Riehemann, M. Palme, T. Peschel, M. Dick, and H. B. Dick, "Presbyopia treatment using a femtosecond laser," *Ophthalmologe* **103**, 1014–1019 (2006).
5. G. Gerten, T. Ripken, P. Breitenfeld, R. R. Krueger, O. Kermani, H. Lubatschowski, and U. Oberheide, "In vitro and in vivo investigations on the treatment of presbyopia using femtosecond lasers," *Ophthalmologe* **104**, 40–46 (2007).
6. C. P. Cain, R. J. Thomas, G. D. Noojin, D. J. Stolarski, P. K. Kennedy, G. D. Buffington, and B. A. Rockwell, "Sub-50-fs laser retinal damage thresholds in primate eyes with group velocity dispersion, self-focusing and low-density plasmas," *Graefes Arch. Ophthalmol.* **243**, 101–112 (2005).
7. V. V. Lozovoy, I. Pastirk, and M. Dantus, "Multiphoton intrapulse interference. IV. Ultrashort laser pulse spectral phase characterization and compensation," *Opt. Lett.* **29**, 775–777 (2004).
8. V. V. Lozovoy and M. Dantus, "Coherent control in femtochemistry," *Chem. PhysChem.* **6**, 1970–2000 (2005).
9. B. W. Xu, J. M. Gunn, J. M. Dela Cruz, V. V. Lozovoy, and M. Dantus, "Quantitative investigation of the multiphoton intrapulse interference phase scan method for simultaneous phase measurement and compensation of femtosecond laser pulses," *J. Opt. Soc. Am. B* **23**, 750–759 (2006).
10. M. Dantus, V. V. Lozovoy, and I. Pastirk, "MIIPS characterizes and corrects femtosecond pulses," *Laser Focus World* **43**, 101–104 (2007).
11. K. A. Walowicz, I. Pastirk, V. V. Lozovoy, and M. Dantus, "Multiphoton intrapulse interference. 1. Control of multiphoton processes in condensed phases," *J. Phys. Chem. A* **106**, 9369–9373 (2002).
12. A. E. Siegman, *Lasers* (University Science Books, 1986).
13. M. Daimon and A. Masumura, "Measurement of the refractive index of distilled water from the near-infrared region to the ultraviolet region," *Appl. Opt.* **46**, 3811–3820 (2007).
14. S. Diddams and J. C. Diels, "Dispersion measurements with white-light interferometry," *J. Opt. Soc. Am. B* **13**, 1120–1129 (1996).
15. L. G. Cohen, "Comparison of single-mode fiber dispersion measurement techniques," *J. Lightwave Technol.* **3**, 958–966 (1985).
16. I. G. Cormack, F. Baumann, and D. T. Reid, "Measurement of group velocity dispersion using white light interferometry: a teaching laboratory experiment," *Am. J. Phys.* **68**, 1146–1150 (2000).
17. B. W. Xu, Y. Coello, V. V. Lozovoy, D. A. Harris, and M. Dantus, "Pulse shaping of octave spanning femtosecond laser pulses," *Opt. Express* **14**, 10939–10944 (2006).
18. A. G. Van Engen, S. A. Diddams, and T. S. Clement, "Dispersion measurements of water with white-light interferometry," *Appl. Opt.* **37**, 5679–5686 (1998).
19. A. H. Harvey, J. S. Gallagher, and J. Sengers, "Revised formulation for the refractive index of water and steam as a function of wavelength, temperature and density," *J. Phys. Chem. Ref. Data* **27**, 761–774 (1998).
20. X. H. Quan and E. S. Fry, "Empirical-equation for the index of refraction of seawater," *Appl. Opt.* **34**, 3477–3480 (1995).
21. R. W. Austin and G. Halikas, "The index of refraction of seawater, Report SIO Reference 76-1" (Scripps Institution of Oceanography, San Diego, 1976).
22. D. X. Hammer, A. J. Welch, G. D. Noojin, R. J. Thomas, D. J. Stolarski, and B. A. Rockwell, "Spectrally resolved white-light interferometry for measurement of ocular dispersion," *J. Opt. Soc. Am. A* **16**, 2092–2102 (1999).
23. D. A. Atchison and G. Smith, "Chromatic dispersions of the ocular media of human eyes," *J. Opt. Soc. Am. A* **22**, 29–37 (2005).
24. R. Navarro, J. Santamaria, and J. Bescos, "Accommodation-dependent model of the human-eye with aspherics," *J. Opt. Soc. Am. A* **2**, 1273–1281 (1985).
25. Y. Le Grand, *Form and Space Vision* (Indiana U. Press, 1967).